Title	Novel Techniques to Reduce Performance Sensitivity to Spatial Correlation and Timing Offset in Space-Time Coded MIMO Turbo Equalization
Author(s)	VESELINOVIC, Nenad; MATSUMOTO, Tadashi; SCHNEIDER, Christian
Citation	IEICE Transactions on Communications, E88-B(4): 1594-1601
Issue Date	2005-04-01
Type	Journal Article
Text version	publisher
URL	http://hdl.handle.net/10119/4680
Rights	Copyright (C)2005 IEICE. N.Veselinovic, T. Matsumoto and C. Schneider, IEICE Transactions on Communications, E88-B(4), 2005, 1594-1601. http://www.ieice.org/jpn/trans_online/
Description	

PAPER

Novel Techniques to Reduce Performance Sensitivity to Spatial Correlation and Timing Offset in Space-Time Coded MIMO Turbo Equalization

Nenad VESELINOVIC[†a)], *Nonmember*, Tadashi MATSUMOTO[†], *Member*, and Christian SCHNEIDER[††], *Nonmember*

SUMMARY   Spatial correlation among antenna elements both at transmitter and receiver sides in MIMO communications is known to have a crucial impact on system performances. Another factor that can severely degrade receiver performances is the timing offset relative to the channel delay profile. In this paper we derive a novel receiver for turbo MIMO equalization in space-time-trellis-coded (STTrC) system to jointly address the problems described above. The equalizer is based on low complexity MMSE filtering. A joint detection technique of the several transmit antennas is used to reduce the receiver's sensitivity to the spatial correlation at the transmitter and receiver sides. Furthermore, only the significant portion of the channel impulse response (CIR) is taken into account while detecting signals. The remaining portion of CIR is regarded as the unknown interference which is effectively suppressed by estimating its covariance matrix. By doing this the receiver's complexity can be reduced since only a portion of the CIR has to be estimated and used for signal detection. Furthermore, by suppressing the interference from the other paths outside the equalizers coverage the receiver's sensitivity to the timing offset can be reduced. The proposed receiver's performance is evaluated using field measurement data obtained through multidimensional channel sounding. It is verified through computer simulations that the performance sensitivity of the joint detection-based receiver to the spatial correlation is significantly lower than with the receiver that detects only one antenna at a time. Furthermore, the performance sensitivity to the timing offset of the proposed receiver is shown to be significantly lower than that of the receiver that ignores the existence of the remaining multipath CIR components.

key words: *turbo equalization, space-time coding, MIMO, MMSE, timing offset, cochannel interference*

1.   Introduction

Signal transmission and reception for communications using multiple transmit and receive antennas over an multiple-input-multiple-output (MIMO) channel is one of the most promising approaches to increasing the link capacity and achievable data rates [1]. Two key approaches have been developed recently to make effective use of the benefits of the MIMO channels. The first one is spatial multiplexing, an example of which is Bell-Labs-Layered-Space-Time-Architecture (BLAST) [2]. It aims at approaching the channel outage capacity. Another scheme that combines the benefits of transmit diversity and channel coding is space-time-trellis-coding (STTrC) [3]. Some recent developments

combine the benefits of the above two approaches [4].

To fully exploit the benefits of broadband frequency selective channels using single carrier signalling, cost efficient implementation of the equalization part of receiver is a key issue. Furthermore, to well utilize the capacity merit of multipath channels turbo processing has been proposed [5], which turns the detrimental effects of the multipath channel into a diversity gain. Recently, MMSE-based turbo-equalization has attracted considerable attention due to the possibilities for adaptive implementation [6] and even further complexity reductions [7].

Iterative equalization with STTrC-codes has been introduced in [8], where the optimal MAP equalizer is used. In this paper, we extend the MMSE-based turbo equalization of [6], [9], [10] to the detection of STTrC-coded signals. A receiver derivation is given for the general case where $n_0 \in \{1, \ldots, N_T\}$ transmit antennas are jointly detected. The receiver is further modified so that only the significant part of the channel impulse response (CIR) is taken into account in the detection process, while the remaining part of CIR is regarded as the unknown interference and it is suppressed using a covariance estimation technique. The performance of the receiver is evaluated using field measurement data, obtained through multidimensional channel sounding. Performance sensitivity to the spatial correlation at the transmitter and receiver sides is evaluated for the two receivers that detect one and all transmit antennas' signals at a time, respectively. The performance sensitivity to the timing offset is evaluated for the receivers that suppress the interference coming from the remaining portion of the CIR and for the one that ignores it.

The rest of the paper is organized as follows. Section 2 describes the system model assumed in this paper. Section 3 presents the proposed receiver, and its special cases for which either one antenna or all transmit antennas are detected simultaneously. Section 4 describes the use of channel measurement data for performance evaluation. Sections 5 and 6 present numerical results and discussions. The paper is concluded in Sect. 7.

2.   System and Received Signal Model

Figure 1 describes the system model assumed in this paper. The bit information sequence $c(i)$, $i = 1, \ldots, Bk_0$ to be trans-

---

Fig. 1 System model.

mitted is encoded using a rate k_0/N_T STTrC code, where N_T and B are the numbers of transmit antennas and frame length in symbols, respectively. The encoded sequences $b(i) \in Q$, $i = 1, \ldots, BN_T$ are first grouped into B blocks of N_T symbols, where $Q = \{\alpha_1, \ldots, \alpha_{2^{k_0}}\}$ denotes the modulation alphabet assumed to be Mary-phase-shift-keying (M-PSK). However, it is straightforward to extend the receiver derivations to the quadrature-amplitude-modulations (QAM). The coded sequence is then interleaved so that the positions within the blocks of length N_T remain unchanged but the positions of the blocks themselves are permuted within the frame according to the interleaver pattern. Thereby, the rank properties of the STTrC codes are preserved [11]. The interleaved sequences are then headed by the training sequences consisting of TN_T symbols. The entire frame is serial-to-parallel converted, resulting in the sequences $b^{(n)}(i)$, $n = 1, \ldots, N_T$, $i = 1, \ldots, B + T$, which are transmitted with N_T transmit antennas over frequency selective channel.

After coherent demodulation in the receiver, the signals from each of N_R receive antennas are sampled in the time domain to capture the multipath components. Observing the signals from different transmit antennas as the virtual users and arranging them in the vector form similarly as in [9], [10] we form the space-time representation of the received signal at the time instant i, given by

$$\mathbf{y}(i) = \underbrace{\mathbf{H}\mathbf{u}(i)}_{\text{desired}} + \underbrace{\mathbf{n}(i)}_{\text{noise}}, \quad i = 1, \ldots, T + B, \tag{1}$$

where $\mathbf{y}(i) \in C^{LN_R \times 1}$ is space-time sampled received signal vector, given by

$$\mathbf{y}(i) = [\mathbf{r}^T(i + L - 1), \ldots, \mathbf{r}^T(i)]^T \tag{2}$$

with $\mathbf{r}(i) \in C^{N_R \times 1}$ being

$$\mathbf{r}(i) = [r_1(i), \ldots, r_{N_R(i)}]^T. \tag{3}$$

L is the number of paths of the frequency selective channel and $r_m(i)$ denotes the signal sample obtained after matched filtering at the mth receive antenna. $\mathbf{H} \in C^{LN_R \times N_T(2L-1)}$ is channel matrix with the form of

$$\mathbf{H} = \begin{bmatrix} \mathbf{H}(0) & \ldots & \mathbf{H}(L-1) & \ldots & \mathbf{0} \\ \vdots & \ddots & & \ddots & \vdots \\ \mathbf{0} & \ldots & \mathbf{H}(0) & \ldots & \mathbf{H}(L-1) \end{bmatrix}$$

and

$$\mathbf{H}(l) = \begin{bmatrix} h_1^{(1)}(l) & \ldots & h_1^{(N_T)}(l) \\ \vdots & \ddots & \vdots \\ h_{N_R}^{(1)}(l) & \ldots & h_{N_R}^{(N_T)}(l) \end{bmatrix},$$

where $h_m^{(n)}(l)$ denotes the l-th path's complex gain between nth transmit antenna and mth receive antenna.

The vector $\mathbf{u}(i) \in Q^{N_T(2L-1) \times 1}$ denotes desired users' sequence, which is defined as

$$\mathbf{u}(i) = [\mathbf{b}^T(i + L - 1), \ldots, \tag{4}$$
$$\mathbf{b}^T(i), \ldots, \mathbf{b}^T(i - L + 1)]^T$$

with

$$\mathbf{b}(i) = [b^{(1)}(i), \ldots, b^{(N_T)}(i)]^T, \tag{5}$$

and $\mathbf{n}(i) \in C^{LN_R \times 1}$ is a vector containing additive white Gaussian noise (AWGN) with covariance $E\{\mathbf{n}(i)\mathbf{n}^H(i)\} = \sigma^2 \mathbf{I}$.

3. Turbo MIMO Equalizers

The receiver first associates the signals from transmit antennas to the groups of length n_0, so that antennas indexed by $n = 1, \ldots, n_0$ belong to the first group, those indexed by $n = n_0 + 1, \ldots, 2n_0$ belong to the second group etc. (see Fig. 1). Obviously, the number of transmit antennas N_T is assumed to be an integer multiple of n_0. Without loss of generality the receiver derivation is presented in Sect. 3.1 for the 1st group of transmit antennas. The derivation is exactly the same for the rest of transmit antenna groups with difference only in indexing. The special cases of $n_0 = 1$ (denoted as rec. 1) and $n_0 = N_T$ (denoted as rec. 2) are considered in more detail in numerical examples.

3.1 SC/MMSE Equalizer Derivation

Starting from (1) we define the received signal that takes into account only a part of channel impulse response of length L_{eff}

$$\mathbf{y}_{eff}(i) = \underbrace{\mathbf{H}_{eff}\mathbf{u}_{eff}(i)}_{\text{desired}}$$
$$+ \underbrace{\mathbf{H}_{I1}\mathbf{u}_{I1}(i) + \mathbf{H}_{I2}\mathbf{u}_{I2}(i)}_{\text{interference}} + \underbrace{\mathbf{n}_{eff}(i)}_{\text{noise}}, \qquad (6)$$

where $\mathbf{y}_{eff}(i)$ is obtained by taking elements of $\mathbf{y}(i)$ that are indexed from PN_T to $(L - E - 1)N_T - 1$, $\mathbf{H}_{eff} \in C^{L_{eff}N_R \times N_T(2L_{eff}-1)}$, $\mathbf{H}_{I1} \in C^{L_{eff}N_R \times N_T(P+L_{eff}-1)}$ and $\mathbf{H}_{I2} \in C^{L_{eff}N_R \times N_T(E+L_{eff}-1)}$ are defined as

$$\mathbf{H}_{eff} = \begin{bmatrix} \mathbf{H}(P) & \dots & \mathbf{H}(L-E-1) & \dots & \mathbf{0} \\ \vdots & \ddots & & \ddots & \vdots \\ \mathbf{0} & \dots & \mathbf{H}(P) & \dots & \mathbf{H}(L-E-1) \end{bmatrix},$$

$$\mathbf{H}_{I1} = \begin{bmatrix} \mathbf{H}(0) & \dots & \mathbf{H}(P-1) & \dots & \mathbf{0} \\ \vdots & \ddots & & \ddots & \vdots \\ \mathbf{0} & \dots & \mathbf{H}(0) & \dots & \mathbf{H}(P-1) \end{bmatrix},$$

and

$$\mathbf{H}_{I2} = \begin{bmatrix} \mathbf{H}(L-E) & \dots & \mathbf{H}(L-1) & \dots & \mathbf{0} \\ \vdots & \ddots & & \ddots & \vdots \\ \mathbf{0} & \dots & \mathbf{H}(L-E) & \dots & \mathbf{H}(L-1) \end{bmatrix},$$

with first P and last E paths not being taken into account, L_{eff} paths taken into account and $L = P + L_{eff} + E$. The vectors $\mathbf{u}_{eff} \in C^{N_T(2L_{eff}-1)\times 1}$, $\mathbf{u}_{I1} \in C^{N_T(L_{eff}+P-1)\times 1}$ and $\mathbf{u}_{I2} \in C^{N_T(L_{eff}+E-1)\times 1}$ are defined as

$$\mathbf{u}_{eff}(i) = [\mathbf{b}^T(i + L_{eff} - 1), \dots, \mathbf{b}^T(i),$$
$$\dots, \mathbf{b}^T(i - L_{eff} + 1)]^T, \qquad (7)$$
$$\mathbf{u}_{I1}(i) = [\mathbf{b}^T(i + L_{eff} + P - 1), \dots, \mathbf{b}^T(i+1)]^T, \qquad (8)$$

and

$$\mathbf{u}_{I2}(i) = [\mathbf{b}^T(i-1), \dots, \mathbf{b}^T(i - L_{eff} - E + 1)]^T. \qquad (9)$$

First, an estimate $\hat{\mathbf{H}}_{eff}$ of the channel matrix $\mathbf{H}_{eff}$ is obtained based on the training sequence $\mathbf{u}_{eff}(i)$, $i = 1, \dots, T$ and soft feedback $\bar{\mathbf{u}}_{eff}(i)$. The soft feedback is obtained by replacing the corresponding elements of $\mathbf{u}_{eff}(i)$ by their soft estimates, defined as

$$\bar{b}^{(n)}(i) = \sum_{q=1}^{2^{k_0}} \alpha_q P_{SISO}^{app}(b^{(n)}(i) = \alpha_q), \qquad (10)$$

where P_{SISO}^{app} denotes *a posteriori* information obtained after SISO decoding. Let us further denote

$$\hat{\mathbf{u}}^{(1,n_0)}(i) = \tilde{\mathbf{u}}_{eff}(i) - \tilde{\mathbf{u}}_{eff}(i) \odot \mathbf{e}^{(1,n_0)}, \qquad (11)$$

where

$$\mathbf{e}^{(1,n_0)} = [\underbrace{0, \dots, 0}_{(L_{eff}-1)N_T}, \underbrace{1, \dots, 1}_{n_0}, \underbrace{0, \dots, 0}_{L_{eff}N_T - n_0}]^T, \qquad (12)$$

and $\odot$ denotes elementwise vector product. The vectors $\tilde{\mathbf{u}}_{eff}(i)$ are obtained by replacing the elements of $\mathbf{u}_{eff}(i)$ by their soft estimates, i.e. an element is given by

$$\tilde{b}^{(n)}(i) = \sum_{q=1}^{2^{k_0}} \alpha_q P_{SISO}^{ext}(b^{(n)}(i) = \alpha_q), \qquad (13)$$

where P_{SISO}^{ext} denotes the extrinsic information obtained after SISO decoding (see [10]). Soft cancellation of inter-symbol interference (ISI) and interference from the antenna sets other than the first one is performed as

$$\hat{\mathbf{y}}^{(1,n_0)}(i) = \mathbf{y}_{eff}(i) - \hat{\mathbf{H}}_{eff}\hat{\mathbf{u}}^{(1,n_0)}(i), \qquad (14)$$
$$i = T + 1, \dots, B + T,$$

The signals $b^{(n)}(i), n = 1, \dots, n_0$ are then jointly detected by filtering the signal $\hat{\mathbf{y}}^{(1,n_0)}(i)$ using a linear MMSE filter whose weighting matrix $\mathbf{W}(i) \in C^{L_{eff}N_R \times n_0}$ satisfies the following criterion

$$[\mathbf{W}(i), \mathbf{A}(i)] = \arg\min_{\mathbf{W},\mathbf{A}} \|\mathbf{W}^H\hat{\mathbf{y}}^{(1,n_0)}(i) - \mathbf{A}^H\boldsymbol{\beta}(i)\|^2. \quad (15)$$

where $\boldsymbol{\beta}(i) \in C^{n_0 \times 1}$ is defined by

$$\boldsymbol{\beta}(i) = [b^{(1)}(i), \dots, b^{(n_0)}(i)]^T, \qquad (16)$$

and $\mathbf{A}(i) \in C^{n_0 \times n_0}$ is a matrix whose diagonal elements satisfy the constraint

$$a_{11}(i) = \dots = a_{n_0 n_0}(i) = 1 \qquad (17)$$

to avoid the trivial solution $[\mathbf{W}(i), \mathbf{A}(i)] = [\mathbf{0}, \mathbf{0}]$. The optimal solution for the nth column $\mathbf{w}^{(n)}(i) \in C^{L_{eff}N_R \times 1}$ of the matrix $\mathbf{W}(i)$ can be shown to be

$$\mathbf{w}^{(n)}(i) = \frac{\mathbf{M}(i)^{-1}\mathbf{h}^{(n)}}{1 + \mathbf{h}^{(n)H}\mathbf{M}(i)^{-1}\mathbf{h}^{(n)}}, \qquad (18)$$

where

$$\mathbf{M}(i) = \hat{\mathbf{H}}_{eff}\boldsymbol{\Lambda}(i)\hat{\mathbf{H}}_{eff}^H + \mathbf{R}(i) - \sum_{n=1}^{n_0} \mathbf{h}^{(n)}\mathbf{h}^{(n)H}, \qquad (19)$$

$\mathbf{h}^{(n)}$ is the $[(L_{eff} - 1)N_T + n]$-th column of the matrix $\hat{\mathbf{H}}$ and $\mathbf{R}(i)$ is the covariance matrix of the interference from the non-significant portion of the CIR and the background noise. The matrix $\boldsymbol{\Lambda}(i)$ is defined as

$$\boldsymbol{\Lambda}(i) = \mathbf{I} - E\{\hat{\mathbf{u}}^{(1,n_0)}(i)\hat{\mathbf{u}}^{(1,n_0)}(i)^H\}$$
$$= \text{diag}\{1 - |[\tilde{\mathbf{u}}(i)]_1|^2, \dots, 1 - |[\tilde{\mathbf{u}}(i)]_{(L_{eff}-1)N_T}|^2, \quad (20)$$
$$\underbrace{1, \dots, 1}_{n_0}, 1 - |[\tilde{\mathbf{u}}(i)]_{(L_{eff}-1)N_T + n_0 + 1}|^2, \dots,$$
$$1 - |[\tilde{\mathbf{u}}(i)]_{(2L_{eff}-1)N_T}|^2\}.$$

Note that Eq. (20) holds only for the M-PSK case, although it is straightforward to extend the receiver derivation to the

more general signal constellations. The optimal values for the non-diagonal elements $a_{n_1 n_2}, n_1 \neq n_2$ of $\mathbf{A}(i)$ is given by

$$a_{n_1 n_2} = \frac{\mathbf{h}^{(n_1)H}\mathbf{M}(i)^{-1}\mathbf{h}^{(n_2)}}{1 + \mathbf{h}^{(n_1)H}\mathbf{M}(i)^{-1}\mathbf{h}^{(n_1)}}. \tag{21}$$

It can be shown that the covariance matrix $\mathbf{R}(i)$ has the following form

$$\mathbf{R}(i) = 2\text{Re}\{\hat{\mathbf{H}}_{eff}\mathbf{\Lambda}_1(i)\mathbf{H}_{I1}^H + \hat{\mathbf{H}}_{eff}\mathbf{\Lambda}_2(i)\mathbf{H}_{I2}^H\} \tag{22}$$
$$+ \mathbf{H}_{I1}\mathbf{H}_{I1}^H + \mathbf{H}_{I2}\mathbf{H}_{I2}^H + \sigma^2\mathbf{I}.$$

Matrices $\mathbf{\Lambda}_1(i)$ and $\mathbf{\Lambda}_2(i)$ are defined as $E\{(\hat{\mathbf{u}}_{eff}(i) - \hat{\mathbf{u}}^{(1,n_0)}(i))\tilde{\mathbf{u}}_{I1}(i)^H\}$ and $E\{(\hat{\mathbf{u}}_{eff}(i) - \hat{\mathbf{u}}^{(1,n_0)}(i))\tilde{\mathbf{u}}_{I2}(i)^H\}$, respectively. In order to exactly calculate $\mathbf{R}(i)$, the matrices $\mathbf{H}_{I1}$ and $\mathbf{H}_{I2}$ (or their estimates) are needed. In this paper, instead, for the practicality reason, we find the time-average approximation of the matrix

$$\hat{\mathbf{R}} = \frac{1}{T}\sum_{i=1}^{T}\|\mathbf{y}_{eff}(i) - \hat{\mathbf{H}}_{eff}\mathbf{u}_{eff}(i)\|^2 \tag{23}$$
$$+ \frac{1}{B}\sum_{i=T+1}^{T+B}\|\mathbf{y}_{eff}(i) - \hat{\mathbf{H}}_{eff}\overline{\mathbf{u}}_{eff}(i)\|^2,$$

which is then used in (19). Assuming that the MMSE filter output $\mathbf{z}(i) \in C^{n_0 \times 1}$ can be viewed as the output of an equivalent Gaussian channel we can write

$$\mathbf{z}(i) = \mathbf{W}^H(i)\hat{\mathbf{y}}^{(1,n_0)}(i) \tag{24}$$
$$= \mathbf{H}_e(i)\boldsymbol{\beta}(i) + \mathbf{\Psi}_e(i),$$

where matrix $\mathbf{H}_e(i) \in C^{n_0 \times n_0}$ contains the channel gains of the equivalent channel defined as

$$\mathbf{H}_e(i) = E\{\mathbf{z}(i)\boldsymbol{\beta}^H(i)\} = \mathbf{W}^H(i)\mathbf{H}_{ML}, \tag{25}$$

with $\mathbf{H}_{ML} = [\mathbf{h}^{(1)}\ldots\mathbf{h}^{(n_0)}]$. The vector $\mathbf{\Psi}_e(i) \in C^{n_0 \times 1}$ is the equivalent additive Gaussian noise with covariance matrix

$$\mathbf{R}_e(i) = E\{\mathbf{\Psi}_e(i)\mathbf{\Psi}_e^H(i)\} \tag{26}$$
$$= \mathbf{W}^H(i)\mathbf{R}_{cov}(i)\mathbf{W}(i) - \mathbf{H}_e(i)\mathbf{H}_e(i),$$

where $\mathbf{R}_{cov}(i) = \hat{\mathbf{H}}_{eff}\mathbf{\Lambda}(i)\hat{\mathbf{H}}_{eff}^H + \mathbf{R}(i)$. The output of the equivalent channel $\mathbf{z}(i)$ and its parameters $\mathbf{H}_e(i)$ and $\mathbf{R}_e(i)$ are passed to the APP block that calculates the *extrinsic* probabilities needed for SISO decoding, as described in Sect. 3.2. The similar procedure is repeated for all N_T/n_0 groups of transmit antennas that are jointly detected. It should be noted that different values of $\mathbf{z}(i)$, $\mathbf{H}_e(i)$ and $\mathbf{R}_e(i)$ are obtained for each group and the dependency of these parameters on the group index is omitted for notation simplicity.

3.2 APP Block and SISO Decoding

The SISO channel decoding algorithm used in this paper is a symbol-level *maximum-a-posteriori* (MAP) algorithm used in [10]. It should be noted that the input required by the decoder is the probability $P(S_i, S_{i+1})$ associated with the transition between two trellis states S_i and S_{i+1} of the STTrC

code. The transition probability can be calculated as

$$P(S_i, S_{i+1}) = P(\beta_k(i) = \mathbf{d}^{i,i+1}) \tag{27}$$
$$= \prod_{n=1}^{N_T} P_{MMSE}^{ext}(b_k^{(n)}(i) = d_n^{i,i+1}),$$

where $\mathbf{d}^{i,i+1} \in C^{N_T \times 1}$ is the vector of encoder outputs that are associated with the trellis state transition (S_i, S_{i+1}). The probabilities $P_{MMSE}^{ext}(b^{(n)}(i) = \alpha_q)$ are extrinsic probabilities obtained by the MMSE detection, which are calculated in the APP block as

$$P_{MMSE}^{ext}(b^{(n)}(i) = \alpha_q)$$
$$= \sum_{\mathbf{f} \in \mathbf{B}^{d_n}} P(\mathbf{z}(i)|\mathbf{f})\left[\prod_{p=1, p\neq n}^{n_0} P_{SISO}^{ext}(b^{(n)}(i) = d_n)\right], \tag{28}$$

for $q = 1, \ldots, 2^{k_0}$ and $n = 1, \ldots, n_0$, where $\mathbf{B}^{d_n} = \{\mathbf{f} \in Q^{n_0 \times 1}|f_n = d_n\}$ and

$$P(\mathbf{z}(i)|\mathbf{f}) = e^{-(\mathbf{z}(i)-\mathbf{H}_e(i)\mathbf{f})^H\mathbf{R}_e^{-1}(i)(\mathbf{z}(i)-\mathbf{H}_e(i)\mathbf{f})}. \tag{29}$$

Based on the transition probabilities $P(S_i, S_{i+1})$ the SISO channel decoder calculates the *a posteriori* probabilities for the symbols $b^{(n)}(i)$, defined as

$$P_{SISO}^{app}(b^{(n)}(i) = \alpha_q) = P(b^{(n)}(i) = \alpha_q|\mathbf{z}(i),$$
$$\mathbf{H}_e(i), \mathbf{R}_e(i), i = T + 1, \ldots, T + B). \tag{30}$$

The decoder extrinsic probability is then calculated as

$$P_{SISO}^{ext}(b^{(n)}(i) = \alpha_q) = \frac{P_{SISO}^{app}(b^{(n)}(i) = \alpha_q)}{\left[P_{MMSE}^{ext}(b^{(n)}(i) = \alpha_q)\right]^Q}, \tag{31}$$

where $0 \leq Q \leq 1$ is an ad hoc parameter that was introduced in [10], [12] where it was shown to significantly improve the iterative receiver's performance. The receiver complexity is dominated by the MMSE part which requires inversion of the matrix $\mathbf{M}(i)$ as well as by the APP block. The overall complexity is therefore $O(\max\{L_{eff}^3 N_R^3, 2^{k_0 n_0}\})$.

4. Performance Evaluation Using Field Measurement Data

Understanding receiver behavior and evaluating its performance in realistic situations is of great importance. The performance obtained using different channel models [13], although being relatively good benchmark, does not accurately reflect many of the practical situations. Therefore, in this paper the realistic channel impulse response is used to evaluate receiver performance. The channel impulse response data is obtained by using multidimensional channel sounder, described in detail in [14], [15]. The measurement campaign took place at the courtyard of the Ilmenau University of Technology, Germany. The measurement route and positions of the transmitter and receiver are illustrated in Fig. 2(a). The transmitter was equipped with uniform-circular-array (UCA) with 16 elements and receiver with
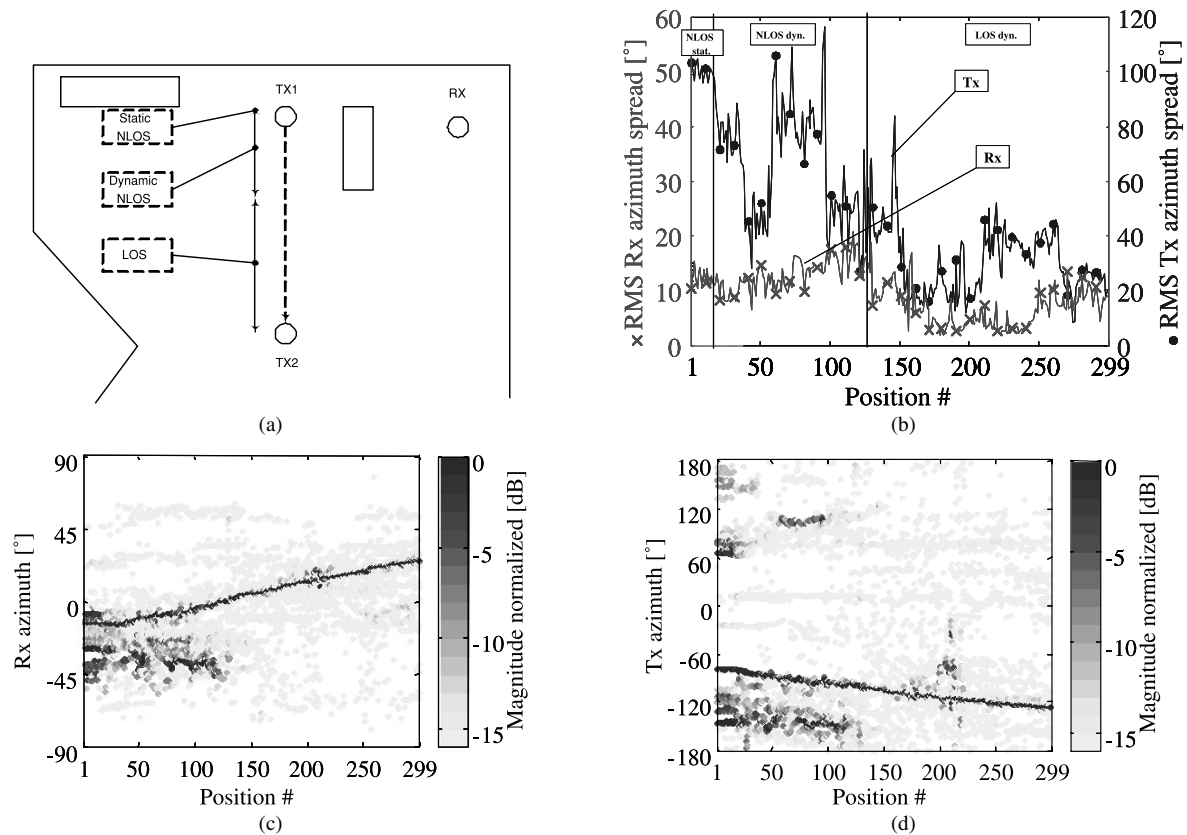
Fig. 2 (a) Map of the measurement area: Transmitter (UCA) is moving along the route, receiver (ULA) is fixed. In the first part of the measurement route the LOS is obstructed by the metal container. Positions $1 - 20$ correspond to S-NLOS, $21 - 125$ to D-NLOS and $126 - 299$ to LOS, (b) Rx and Tx spatial spread vs. position index, (c) angles of arrival at the Rx array vs. position index, (d) angles of departure from the Tx array vs. position index.

uniform-linear-array (ULA) with 8 elements. The measurement bandwidth of channel sounding was 120 MHz. Transmit and receive antenna spacing were $0.5\,\lambda$ and $0.4\,\lambda$ and they were mounted at the heights of 2.1 m and 1.67 m, respectively. The receiver was stationary during measurement, while the transmitter was moving at a walking speed. Three different regions can be distinguished along the route. First, the static non-line-of-site (S-NLOS) region, where transmitter was stationary and the LOS was obstructed by the metal container. Second, the dynamic-NLOS (D-NLOS) region, where the transmitter was moving but the LOS was still obstructed. Third, the LOS region, where the LOS between transmitter and receiver exists. The details of the spatio-temporal structure of the channel in the given measurement area can be found in [15]. Figures 2 (b), (c) and (d) present the estimated spatial spreads and angles of arrival and departure at the transmitter and receiver sides,respectively, obtained by super-resolution estimation algorithm presented in [16].

The 4-state QPSK space-time trellis code with bandwidth efficiency 2 bits/(sHz) and $N_T = 2$, presented in [3] was used at the transmitter. The channel interleaver was random. The assumed symbol rate was 20 Msymb/sec. The signal to be transmitted was upsampled and filtered using a

raised-cosine filter with roll-off factor equal to 0.25 to form a signal whose bandwidth is adjusted to the measurement equipment bandwidth. The upsampled and filtered signal was then convoluted with the measured channel impulse responses to produce the received signal samples. The received signal is again convoluted with the receiver raised-cosine filter and finally downsampled to the original data rate of 20 Msymb/sec. The Log-MAP space-time trellis decoder shown in [17] and [10] was used after MMSE equalization.

5. Numerical Examples

The number of positions for which the measurements were performed was 299. The performance of the proposed receivers is investigated for selected positions out of 299 available. Positions indexed by $1-20$ in the plots in Fig. 2 belong to the S-NLOS region, while those indexed by $21-125$ and $126-299$ belong to the D-NLOS and LOS regions, respectively. The total number of symbol-spaced multipath components L observed after filtering and downsampling at the receiver was equal to 24.

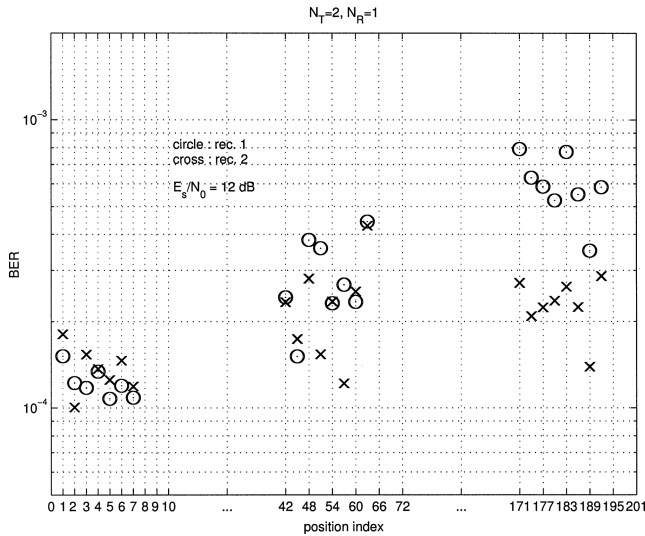**Example 1.** Fig. 3 presents bit-error-rate (BER) performance vs. measurement position index. The perfor-

Fig. 3 BER vs. position index, $(N_T, N_R) = (2, 1)$, $E_s/N_0 = 12$ dB, $Q = 0.5$, $L_{eff} = 11$.

Fig. 4 Symbol-spaced channel impulse responses observed after receive filter and downsampling, position #123 that belongs to D-NLOS region, (a) from transmit antenna 1 to the receive antennas 1, 4 and 7, (b) from transmit antenna 2 to the receive antennas 1, 4 and 7.

mance is evaluated for positions indexed by $1, \ldots, 7$, and $42, 45, \ldots, 63$ and $171, 174, \ldots, 182$ (every third). Effective number L_{eff} of multipath components is kept constant for all snapshots and chosen to be 11. The optimal timing P was determined for each snapshot separately by sliding the timing window along the channel impulse response vector and timing optimality $P = P_{opt}$ was defined such that the total received power contained in a window of length L_{eff} is maximized, as

$$P_{opt} = \arg\max_P \sum_{l=P}^{P+Leff-1} \sum_{m=1}^{N_R} \sum_{n=1}^{N_T} \|h_m^{(n)}(l)\|^2. \qquad (32)$$

The signal power is then controlled so that the total received power for each transmit-receive antenna pair is equal to unity for each position. The antenna elements 1 and 8 of the transmit UCA and the element 1 of the receive ULA were used at the transmitter and receiver sides, respectively, resulting in radio network topology $(N_T, N_R) = (2, 1)$. Simulations for each snapshot are performed until 100 frame errors took place.

Example 2. Figs. 4(a) and (b) present the channel impulse responses from the transmit antenna elements 1 and 8 to each of the receive antenna elements 1, 4 and 7 for the position #123. Without loss of generality this particular snapshot is randomly chosen from the D-NLOS region. Therefore the simulation scenario can be described by $(N_T, N_R) = (2, 3)$. Figure 5 presents BER performance vs. E_s/N_0, for L_{eff} being fixed to 3 with P as a parameter. Thereby, the received signal power totalling over all $L = 24$ paths was used when defining E_s/N_0 in Fig. 5. Simulations for each snapshot were performed until 100 frame errors are collected. It is found that $P = 3$ gives the best performance of the proposed receivers and that value corresponds to offset= 0.
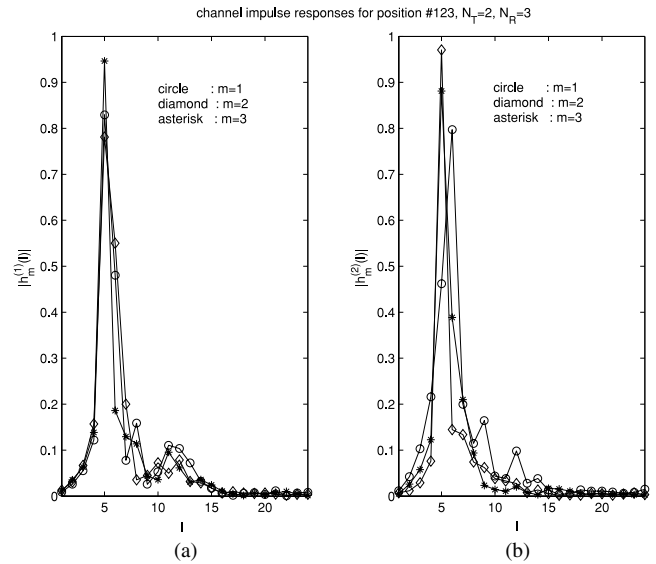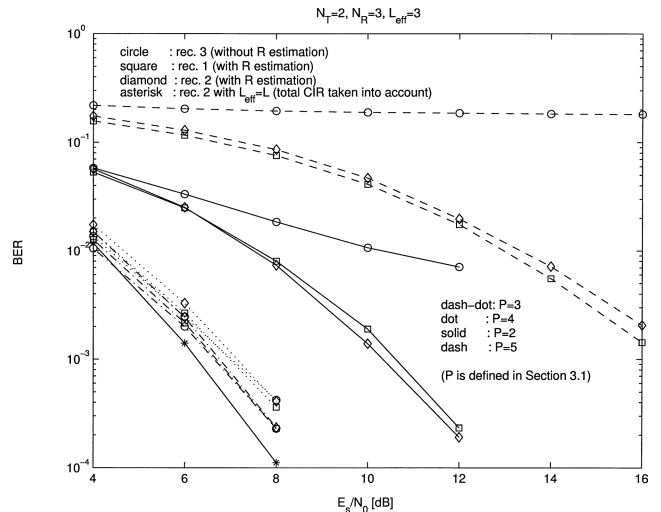

Fig. 5 BER vs. E_s/N_0, comparison of receivers with and without covariance matrix estimation, $(N_T, N_R) = (2, 3)$, $L_{eff} = 3$, $Q = 0.5$.

6. Discussions

It is found in Fig. 3 that the rec. 1's ($n_0 = 1$) performance is much better in the NLOS region than in the LOS region. On the contrary, rec. 2's ($n_0 = 2$) performance is almost constant regardless of the propagation condition. This is due to the larger spatial spread at the transmitter side in the NLOS region (see Fig. 2(b)), resulting in the lower spatial correlation among the transmit antenna elements. Since the rec. 1 performs spatial separation of transmit antenna elements' streams using MMSE filtering, its performance is better in the NLOS case. The rec. 2's superiority is due to the joint detection of signals transmitted using two transmit antenna

elements. Thereby, the separation of two transmit antennas' signals is performed in the APP block itself instead in the MMSE receiver. The improvement achieved by the rec. 2 over the rec. 1 is larger in the LOS region. Therefore, preserving the degrees of freedom of the MMSE receiver by joint detection is more beneficial in the LOS than in the NLOS regions.

In Fig. 5 the receiver's performance sensitivity to the timing offset is presented. The rec. 1 and rec. 2 are compared with another receiver that ignores the existence of the less significant multipath components, with which $\mathbf{R} = \sigma^2 \mathbf{I}$. This receiver is referred to as rec. 3, for notational convenience. It is found in Fig. 5 that the rec. 1 and 2 perform very similarly, due to the fact that the position #123 belongs to the D-NLOS region, where the spatial spread at both the transmitter and the receiver are relatively large. If the synchronism is maintained perfectly (offset= 0) the rec. 1 and rec. 2's performances are almost the same as rec. 3's, since most of the received signal power is concentrated in the significant portion of the channel impulse response, and the energy from the significant portion falls into the equalizer coverage. The performance of the rec. 2 that takes into account the whole CIR is also shown to perform only about 0.5 dB better than the proposed receivers. However, in cases that offset= −1 or offset= 2 the rec. 3's performance is significantly degraded and it plateaus at a certain BER level. At the same time, the receivers which estimate covariance matrix (rec.1 and rec.2) can considerably suppress the remaining interference components asymptotically when the E_s/N_0 becomes large. Thereby, the performance sensitivity to the timing offset is significantly reduced. Note that the E_s/N_0 loss in cases where $P = 2, 4$, and 5 is due to the unequal powers of the selected portions of the CIR for different values of P and constant L_{eff}.

7. Conclusions

A new MMSE-based iterative MIMO equalization algorithm for the STTrC coded systems in frequency selective channels is derived. The proposed algorithm performs joint detection of signals transmitted using several transmit antenna elements in order to reduce the receiver's sensitivity to the spatial spread at the transmitter and receiver side. Furthermore, by using only a significant part of CIR for signal detection purpose, and by suppressing the rest of the CIR using covariance matrix estimation technique the receivers' performance sensitivity to the timing offset can be significantly reduced.

The proposed receiver's performance was tested through computer simulations using field measurement data, obtained through multidimensional channel sounding, for realistic performance evaluation in fields. It has been shown that the receiver's performance sensitivity to the spatial spread can be significantly reduced by performing joint detection of transmit antennas' signals. Furthermore, it has been shown that the receiver which jointly detects transmit antennas' signals can achieve better performance than the

receiver that detects antenna-by-antenna, when the propagation scenario is LOS. It has also been shown that the receiver that aims to suppress interference caused by the nonsignificant CIR components, by estimating their covariance matrix, has significantly lower performance sensitivity to the timing offset, compared to the receiver that ignores the interference.

Acknowledgement

References

[1] E. Telatar, "Capacity of multi-antenna Gaussian channels," European Trans. Telecommun., vol.10, no.6, pp.585–595, Nov.-Dec. 1999.

[2] G. Foschini, "Layered space-time architecture for wireless communication in a fading environment when using multi-element antennas," Bell Labs Tech. J., pp.41–59, Aug. 1996.

[3] V. Tarokh, N. Seshadri, and A.R. Calderbank, "Space-time codes for high data rate wireless communication: Performance criterion and code construction," IEEE Trans. Inf. Theory, vol.44, no.2, pp.744–765, 1998.

[4] A.O. Berthet and R. Visoz, "Iteraive decoding of concatenated layered space-time trellis codes on MIMO block fading multipath AWGN channel," IEEE Trans. Commun., vol.51, no.6, pp.940–952, June 2003.

[5] S.L. Ariyavisitakul, "Turbo space-time processing to improve wireless channel capacity," IEEE Trans. Commun., vol.48, no.8, pp.1347–1359, Aug. 2000.

[6] X. Wang and H.V. Poor, "Iterative (turbo) soft interference cancellation and decoding for coded CDMA," IEEE Trans. Commun., vol.47, no.7, pp.1046–1061, July 1999.

[7] K. Kansanen and T. Matsumoto, "A computationally efficient MIMO turbo-equaliser," Proc. IEEE Veh. Technol. Conf. (VTC), Jeju, Korea, April 2003.

[8] G. Bauch, A.F. Naguib, and N. Seshadri, "MAP equalization of space-time coded signals over frequency selective channels," Proc. IEEE Wireless Commun. and Networking Conf. (WCNC), pp.261–265, New Orleans, LA, Sept. 1999.

[9] T. Abe and T. Matsumoto, "Space-time turbo equalization in frequency-selective MIMO channels," IEEE Trans. Veh. Technol., vol.52, no.3, pp.469–475, May 2003.

[10] B. Lu and X. Wang, "Space-time code design in OFDM systems," Proc. IEEE Global Telecommun. Conf. (GLOBECOM), pp.1000–1004, San Francisco, CA, Nov.–Dec. 2000.

[11] A.F. Naguib, V. Tarokh, N. Seshadri, and A.R. Calderbank, "A space-time coding modem for high-data-rate wireless communications," IEEE J. Sel. Areas Commun., vol.16, no.8, pp.1459–1478, 1998.

[12] C. Douillard, C.M. Jezequel, C. Berrou, A. Picart, P. Didier, and A. Glavieux, "Iterative correction of intersymbol interference: Turbo-equalisation," European Trans. Telecommun., vol.6, no.5, pp.507–511, Sept. 1995.

[13] J.P. Kermoal, L. Schumacher, K. Pedersen, P.E. Mogensen, and

F. Frederiksen, "A stochastic MIMO radio channel model with experimental validation," IEEE J. Sel. Areas Commun., vol.20, no.6, pp.1211–1226, Aug. 2002.

[14] www.channelsounder.de

[15] C. Schneider, U. Trautwein, T. Matsumoto, and R. Thomä, "Dependency of turbo MIMO equalizer performances on spatial and temporal multipath channel structure—A measurement based evaluation," Proc. IEEE Veh. Technol. Conf. (VTC), Jeju, Korea, April 2003.

[16] R. Thomä, D. Hampicke, A. Richter, G. Sommerkorn, and U. Trautwein, "MIMO measurement for double-directional channel modeling," European Trans. Telecommun., vol.12, no.5, pp.427–438, Sept. 2001.

[17] S. Benedetto, G. Montorsi, D. Divsalar, and F. Pollara, "Soft-in-soft-output APP module for iterative decoding of concatenated codes," IEEE Commun. Lett., vol.1, no.1, pp.22–24, Jan. 1997.

Christian Schneider received his Diploma degree in electrical engineering from the Technische Universität Ilmenau, Ilmenau, Germany in 2001. He is currently pursuing the Dr.-Ing. degree with the Electronic Measurement Research Lab of the Institute of Communications and Measurement Engineering at the Technische Universität Ilmenau. His research interests include space-time signal processing, turbo techniques, multi dimensional channel sounding, channel characterization and channel modelling.

Nenad Veselinovic received his M.S. and Ph.D. degrees in electrical engineering from University of Belgrade, Serbia and Montenegro in 1999 and University of Oulu, Finland in 2004, respectively. Since 2000 he has been with the Centre for Wireless Communications, University of Oulu, Finland where he is currently working as a Research Scientist. Mr. Veselinovic's main research interests are statistical signal processing and receiver design for broadband wireless communications. He is a member of IEEE.

Tadashi Matsumoto received his B.S., M.S., and Ph.D. degrees in electrical engineering from Keio University, Yokohama-shi, Japan, in 1978, 1980 and 1991, respectively. He joined Nippon Telegraph and Telephone Corporation (NTT) in April 1980. From April 1980 to January 1991, he researched signal transmission techniques such as modulation/demodulation, error control, and radio link design schemes for 1st and 2nd-generation mobile communications systems. In July 1992, he transferred to NTT DoCoMo, where he researched Code Division Multiple Access (CDMA) techniques. From 1992 to 1994, he served as a part-time lecturer at Keio University. In April 1994, he transferred to NTT America, where he served as a Senior Technical Advisor in the NTT-NEXTEL Communications joint project. In March 1996, he returned to NTT DoCoMo, and he was appointed a head of radio signal processing laboratory at NTT DoCoMo, where he researched adaptive signal processing, MIMO Turbo signal detection, interference cancellation, and space-time coding techniques for broadband mobile communications. In May 2002, he moved to University of Oulu, Finland, where he is a professor at Center for the Wireless Communications. Presently, he is serving as a board-of-governor of the IEEE VT Society for a term from Jan. 2002 to Dec. 2004.